energies

MDPI

Case Report

Application of Photovoltaic Systems for Agriculture: A Study on the Relationship between Power Generation and Farming for the Improvement of Photovoltaic Applications in Agriculture

Jaiyoung Cho [1,*], Sung Min Park [2], A Reum Park [1], On Chan Lee [3], Geemoon Nam [3] and In-Ho Ra [4,*]

1 Wongwang Electric Power Co., 243 Haenamhwasan-ro, Haenam-gun 59046, Jeollanamdo, Korea; jereint35@naver.com
2 Department of Horticulture, Kangwon National University, Chuncheon 24341, Jeollanamdo, Korea; parksm@kangwon.ac.kr
3 SM Software, 1175, Seokhyeon-dong, Mokposi 58656, Jeollanamdo, Korea; oc.lee@smsoft.co.kr (O.C.L.); chrisnam0315@gmail.com (G.N.)
4 Department of Information and Communication Technology, Kunsan National University, Gunsan 54150, Jeollabuk-do, Korea
* Correspondence: pra0200@naver.com (J.C.); ihra@kunsan.ac.kr (I.-H.R.); Tel.: +82-62-384-9118 (J.C.); +82-63-469-4697(I.-H.R.)

Received: 29 August 2020; Accepted: 11 September 2020; Published: 15 September 2020

Abstract: Agrivoltaic (agriculture–photovoltaic) or solar sharing has gained growing recognition as a promising means of integrating agriculture and solar-energy harvesting. Although this field offers great potential, data on the impact on crop growth and development are insufficient. As such, this study examines the impact of agriculture–photovoltaic farming on crops using energy information and communications technology (ICT). The researched crops were grapes, cultivated land was divided into six sections, photovoltaic panels were installed in three test areas, and not installed in the other three. A 1300 × 520 mm photovoltaic module was installed on a screen that was designed with a shading rate of 30%. In addition, to collect farming-cultivation-environment data and to analyze power generation, sensors for growing environments and wireless-communication devices were used. As a result, normal modules generated 25.2 MWh, bifacial modules generated 21.6 MWh, and transparent modules generated 25.7 MWh over a five-month period. We could not find a difference in grape growth according to the difference of each module. However, a slight slowing of grape growth was found in the experiment group compared to the control group. Nevertheless, the sugar content of the test area of the grape fruit in the harvest season was 17.6 Brix on average, and the sugar content of the control area was measured at 17.2 Brix. Grape sugar-content level was shown to be at almost the same level as that in the control group by delaying the harvest time by about 10 days. In conclusion, this study shows that it is possible to produce renewable energy without any meaningful negative impact on normal grape farming.

Keywords: solar sharing; agriculture–photovoltaic; integrating agriculture; solar-energy harvesting

1. Introduction

The Korean government's Ministry of Trade, Industry, and Energy (MOTIE) recently announced the 2030 Energy New Industry Expansion Strategy Plan, which aims to supply 20% of electricity from renewable-energy sources by 2030, thereby increasing photovoltaic (PV) power-generation capacity

from 5.7 to 35.5 GW. The availability of usable land, however, poses a challenge, since 63% of the existing PV plants are currently built in rural areas, encroaching on farmland and fields. Securing land six times larger than the current mass to implement extra PV plants is also impossible without consuming more farmland. Under these circumstances, the government, power producers, and farmers are all showing great interest in agrivoltaic farming, a method that combines PV generation and conventional agriculture. Accordingly, this maximizes land use by utilizing arable land for the coexistence of power generation and crop cultivation. However, since agrivoltaic systems are under-researched, current data on the effects on crops under an agrivoltaic system, correlations with power-generation levels, and economic feasibility are insufficient. Therefore, this study provides data on power generation and crop growth using information and communications technology (ICT), and analyses of the characteristics and economics of an agrivoltaic farm.

As the number of PV power plants has increased globally, there have been concerns regarding their ability to cause environmental disruption. As an alternative, in 2004, Nagashima Akira introduced the concept of solar sharing, where PV power generation and crop cultivation are simultaneously performed.

Solar sharing, also described as an agrivoltaic (agriculture–photovoltaic) system, is currently being actively researched as a new alternative to conventional PV plants.

The effect of onion growth under the shadow of solar panels was studied. In this study, two types of PV panel distribution (checkerboard and straight-line) were tested, each occupying 12.9% of the roof area. As a result of the study, the generated electricity by the PV array of the two types was similar. The straight-line PV array, however, decreased the dry-matter weight (DW) and fresh weight (FW) of onions compared to the checkerboard PV array [1].

In a study where a solar module was installed over 50% of the roof area of a greenhouse, the result showed that solar radiation inside the greenhouse was reduced by 64% annually on average [2]. Auxiliary lighting that supplies electricity without exceeding the energy produced by the PV module was insufficient to produce onions, and profits were lower than the cost of heating and lighting [2]. Onion farms with 50% solar-module shade had a negative impact on agriculture, which led to the study of a shading rate of about 30%.

Kuo YC studied the optical properties of greenhouses that had various types of PV modules (crystalline light-through, colorful, and see-through modules) installed, and reported that it is possible to make spectrum and light distributions ideal for plant growth through the selection of appropriate modules [3].

In modern precision farming, the need for real-time monitoring of crop-growth-parameter data, including microclimate, soil temperature, soil moisture, solar radiation, and leaf wetness, necessitates the use of wireless sensors and robot agents [4] on fields that operate on rechargeable batteries with solar panels. Such sensors have been successfully used in greenhouses for monitoring the comfort ratio of microclimate parameters [5], where artificial lights are available, and shadowing is not considered to be a limiting factor.

In the checkerboard pattern, the presence of solar panels on the roof of a tomato greenhouse with 10% shade did not significantly affect tomato yield. Farmers in warm climates can produce electricity by installing solar panels on 10% of the roofs of tomato greenhouses without harming agricultural production during the spring–summer crop cycle [6]. On the basis of these research results, we designed a shading rate higher than 10%.

Studies on farm-type photovoltaic-power-generation systems have so far focused on minimizing the negative effects of photovoltaic systems on the cultivation of crops by installing photovoltaic panels at a height of more than 4 m from the ground and a less than 30% shading rate. Figure 1 is a farm-type solar-power plant installed by the Wongwang electric power company (WEPCO) in the city of Naju, Republic of Korea. Figure 1 shows an example of installing solar power in a cabbage farm using a half module [7–16].

Figure 1. Farm-type photovoltaic-power-generation system.

On the other hand, we studied how to use a photovoltaic system as part of a crop-cultivation environment, which was different from the conventional approach whereby the negative effects of a photovoltaic system on crop cultivation are minimized [17–28]. Plants such as grapes and peppers increase the incidence of pests and deteriorate yield and productivity when they are subjected to rainfall during the growth process. Therefore, an umbrella-shaped facility using a photovoltaic system was installed to prevent raindrops from hitting the crops, shown in Figure 2 [29–32].

Figure 2. Rain-hit-protection facility in a grape farm.

In this study, the solar-power-generation system replaced the rain-hit-protection facility, and a model was developed to use as a rain-hit-protection construction to reduce maintenance costs and increase farmers' revenue by additional profit from photovoltaic generation. The main contribution of this research was to examine the effects of agrivoltaic farming on power-generation level and crop growth above 30% shading, as shown in Figure 3. We studied whether there was any impact on

crop productivity under shading rates greater than 12.9% and at 10% which were used from previous studies on onions and tomatoes, respectively [1,6].

Figure 3. Rain-hit-protection solar facility in a grape farm.

Crop-growth monitoring and a smart-farming system were implemented to gather data using various sensors. The collected data were used as a basis to monitor and evaluate the impact of agrivoltaic generating on grape-crop growth and sugar content.

2. Materials and Methods

2.1. Solar-Generation System

To study the crop-growth environment in a rain-hit-protection facility, a test bed (37°15′54.9″ N 126°29′15.8″ E) was installed in Ongjin-Gun, Republic of Korea, where rain-shield cultivation is popular.

The structure of the photovoltaic system was designed to be similar to the existing rain-shield system in order to compare the cultivation environment and product quality under homogeneous conditions. Structure span was 2400 mm, and height was 2000 mm above the ground. The upper structure had a 15° angle to force the rain to drop in a specific direction and braces were implemented 570 mm above ground to control structure deflection and wind load. To use the photovoltaic system as a rain shield, acryl panels were installed on top of the structure that formed the 15° angle. The shading rate of the solar panel was designed to be 30% of the total roof area. The solar panels were fitted onto the roof using a checkerboard pattern, as shown in Figure 4.

To analyze the difference in cultivation environment due to module shading, normal solar panels and transparent panels were installed. In addition, to increase power-generation efficiency, normal and bifacial modules were installed. Module sizes were 1476 × 666, 1524 × 686, and 1476 × 780 mm^2, which are approximately half the size of a general module. In the 1800 m^2 test bed, 600 m^2 was used to install each type of module, thus forming 3 types of test bed. Figures 5 and 6 shows aerial photographs and section views of a farm with three installed panels. The aerial photographs and drawings of the farm show that Section B faces south, Section D is southeast, and Section F is southwest.

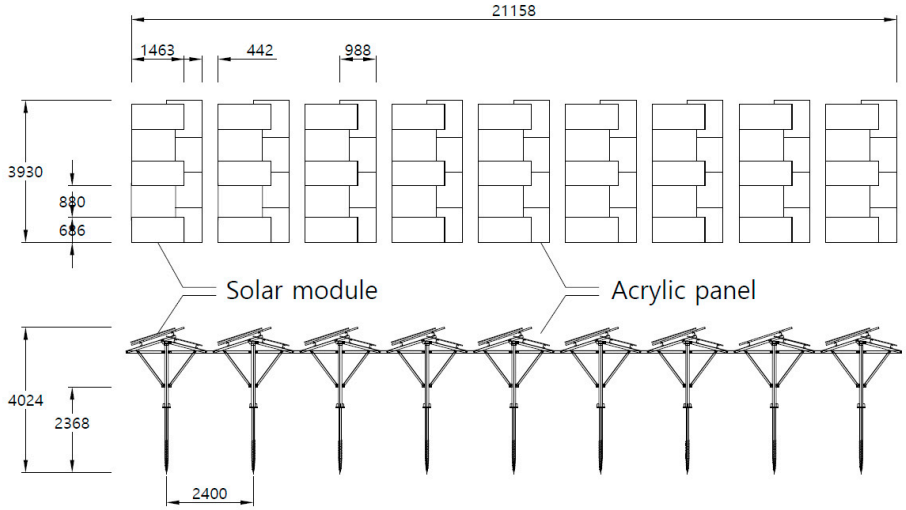

Figure 4. Structure of photovoltaic system.

Figure 5. Aerial photo of 3 types of installed panels.

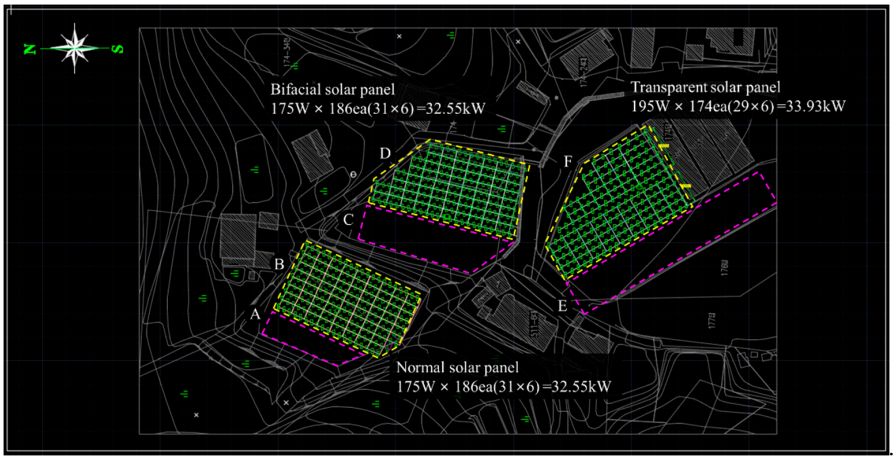

Figure 6. Sections of 3 types of installed panels. A, normal control site; B, normal solar-panel site; C, bifacial control site; D, bifacial solar-panel site; E, transparent control site; and F, transparent solar-panel site.

The installation capacity of each type of module was 33 kW, and the total solar-power capacity of the test bed was 99 kW. Generally, photovoltaic modules were installed facing southward, but the

direction of the modules for agrivoltaic systems changed depending on the shape of the farm ridge and furrow. Therefore, not all modules were facing in the same direction. Section B maintained a south direction by a turnable type of solar system on top of a rain-hit facility, but it is vulnerable to typhoons and was more costly than the solar systems used Sections D and F. Sections D and F were installed as roof built-in types to compare energy generation. Figure 7 shows the 3 types of solar-system structures in the experiment site.

Section B **Section D** **Section F**

Figure 7. Three types of solar panels. **B**, normal type; **D**, bifacial type; **F**, transparent type.

As described above, 3 types of photovoltaic power plant were constructed in the test bed. Then, cultivation environment and crop quality were compared with the control site (Sections A, C, and E).

2.2. Smart-Farming System

Sensors in the facility were installed to monitor the growth environment in the solar-power-generation system for rain-hit-protection facilities. The sensors were an illuminance sensor (BH1750FVI, ROHM SEMICONDUCTOR, Kyoto, Japan), solar-irradiance sensor (NHFS15, Wuhan Ahongke Nenghui Technology Co., Wuhan, China), temperature sensor (DS18B20, Maxim Integrated, San Jose, CA, USA), CO_2 sensor (MH-Z16, Zhengzhou Winsen Electronics Technology CO., Zhengzhou, China), and a temperature and humidity sensor (AM2305, AOSONG, Guangzhou, China).

Sensors were installed in Sections C and D. The growth environment was monitored from April 2019 to December 2019. Grapes germinate in April, the coloration and growth of the fruit occur until July, and grapes are harvested in August. The growth-environment monitoring during germination, fruiting, coloration, and harvesting is crucial, as changes in the growth environment during these periods could cause major changes in crop quality.

Figure 8 shows sensor locations in the experimental site, Section D. Data measurements by the sensors were stored on the server every minute. Data with electric values from other sensors were acquired from the solar inverter.

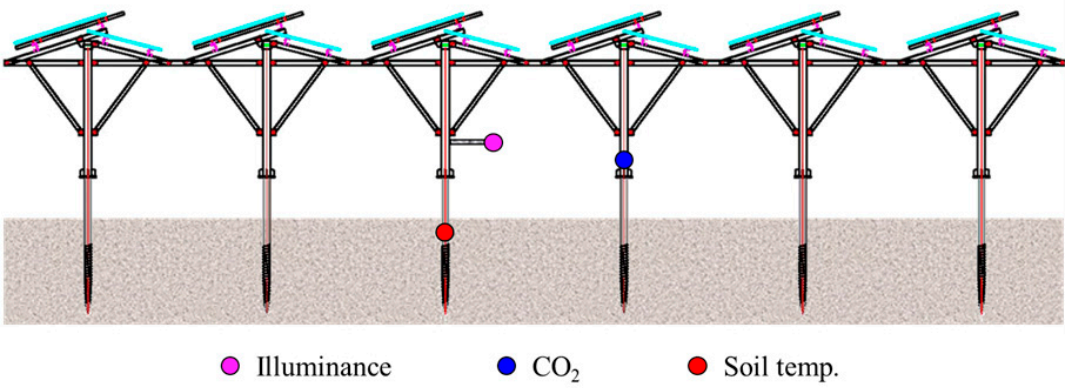

Figure 8. Data-collection process.

The measured data by each sensor and inverter were stored in a web server by TCP/IP communication, as illustrated in Figure 9. Smart farming system, in turn, is enabled by the growth environment data from the web server, which provides an automated schedule to control the amount of water supply, as shown in Figure 10. Figure 11 represents the web page for monitoring the integrated management system. Overall, these systems allow us to check the amount of power generated by the inverter, the crop environment, and cumulative history on power generation.

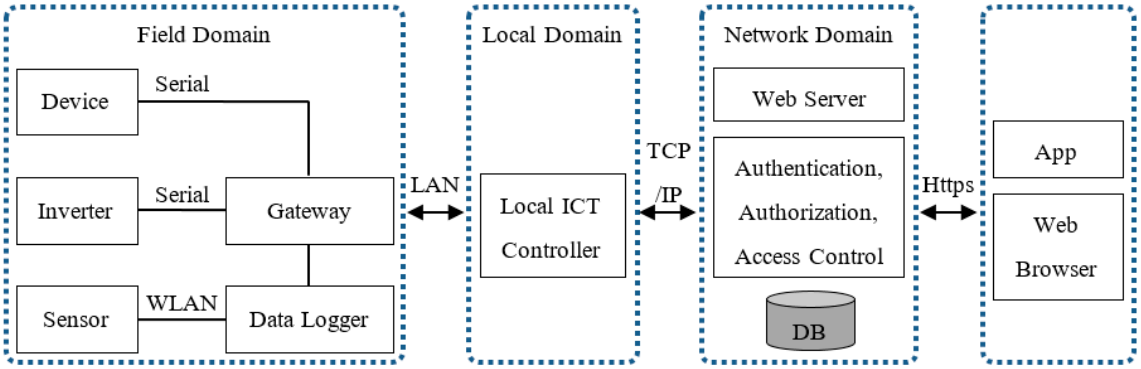

Figure 9. Flow chart for storage in a web server by TCP/IP communication.

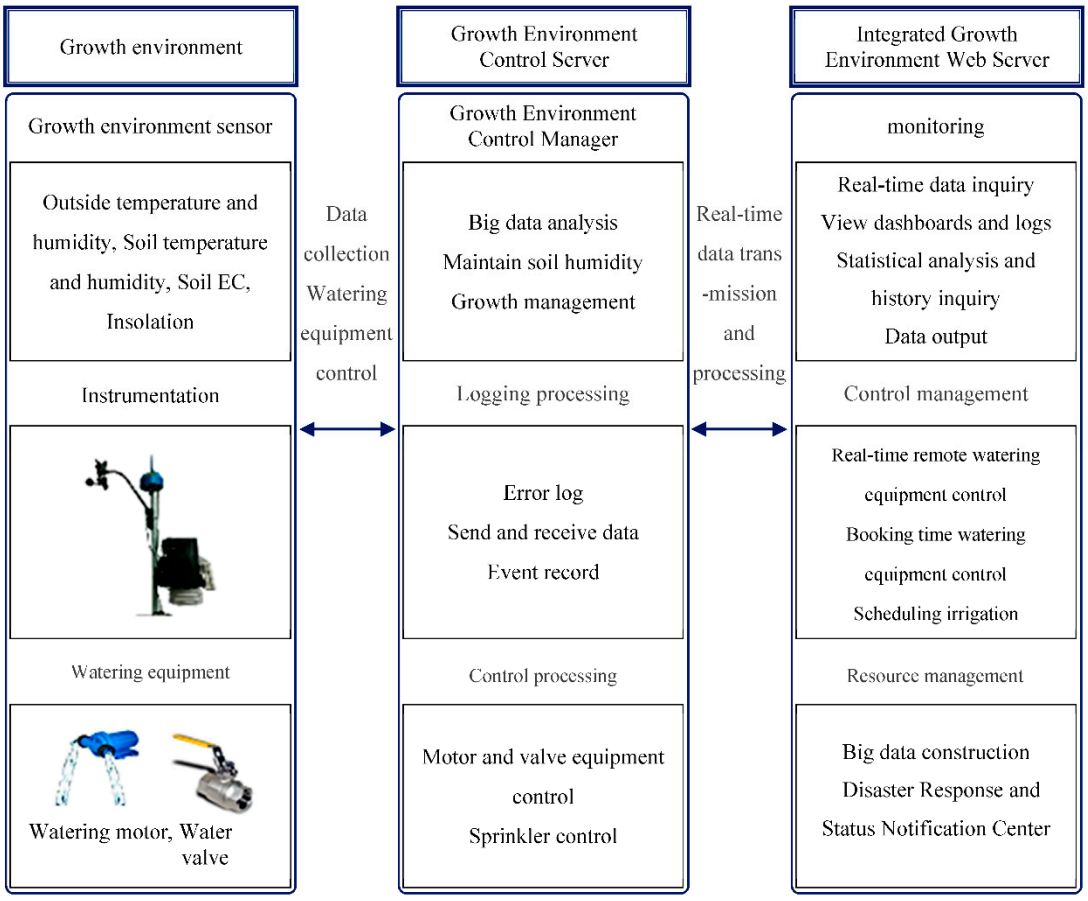

Figure 10. Smart-farming-system diagram.

Figure 11. Integrated management system for agrivoltaics.

Figures 12–14 show detailed characteristics of three types of installed photovoltaic (PV) panels.

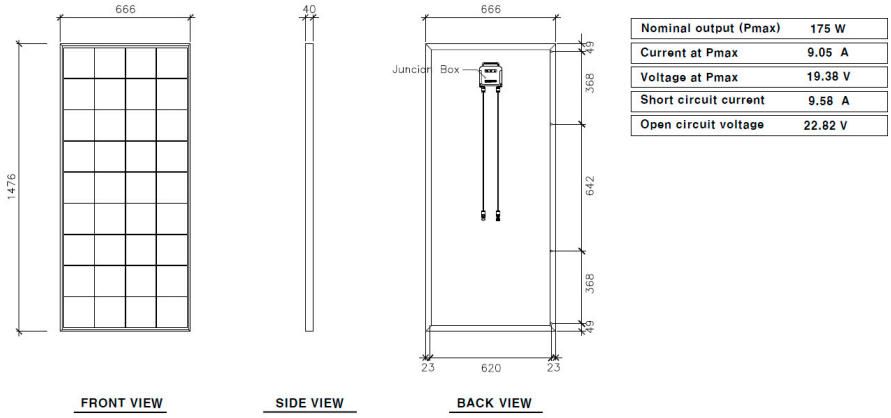

Figure 12. Normal-panel specification (Section B).

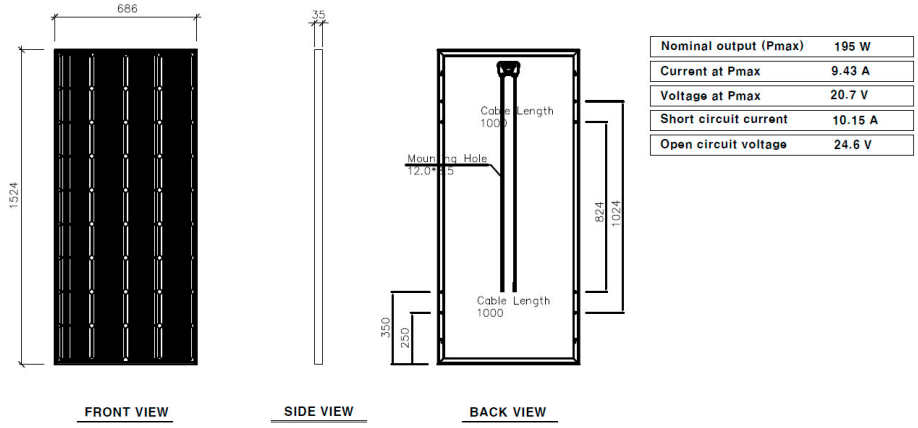

Figure 13. Bifacial-panel specification (Section D).

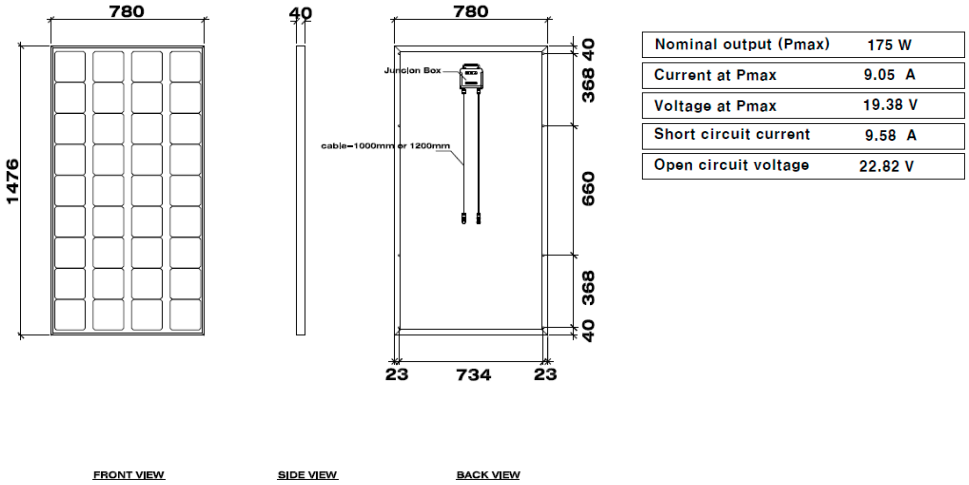

Figure 14. Transparent-panel specification (Section F).

3. Results and Discussion

3.1. Power-Generation Analysis

The normal, bifacial, and transparent solar-panel modules were connected to three inverters, and real-time power-generation data were uploaded to the server. The photovoltaic system was a grid-connected type, and the inverter was 34 kW. Photovoltaic-generation data during the five months were collected, and results are shown in Table 1. Bifacial modules were expected to show higher power-generation efficiency than that of normal modules, but power generation was higher in the normal modules installed in the south direction than that in bifacial modules installed in the southeast direction. In addition, the power generation of normal and transparent modules installed in the south direction was similar, but the generation peak time was different due to the difference in the direction of module installation. Figure 15 shows the electricity-generation pattern of each type of panel on 18 July 2019. It shows that the power-generation efficiency was determined by the module installation direction rather than the module performance in this study. The reason for the different peak times of generation was that Section B was facing south, D southeast, and F southwest, as aerial photographs and drawings of the entire vineyard show.

Table 1. Agricultural-solar-plant proceeds.

Contents	Unit	April	May	June	July	August	Total
Days	Days	30	31	30	31	31	153
PV energy	kWh	8978	11,454	12,393	10,426	12,631	55,882
Electric price (SMP)	USD/kWh	0.117	0.094	0.093	0.094	0.1	0.1
Sales income	USD	1057	1081	1153	985	1270	5551
PV exchange time	hours	3.02	3.73	4.17	3.40	4.12	3.69

In the case of plant agrivoltaic systems, like grapes, most crops have a fixed cultivation direction. Thus, the priority needs to be decided at the design stage between the furrow cultivation direction and power-generation efficiency.

Figure 16 shows the power-generation data of three different PV types. The normal module generated 25.2 MWh, the bifacial module generated 21.6 MWh, and the transparent module generated 25.7 MWh over seven months. The power generation of the transparent module was the best, but this was due to the direction of the module. Therefore, it cannot be concluded that the power-generation performance of the transparent module was superior to that of other modules.

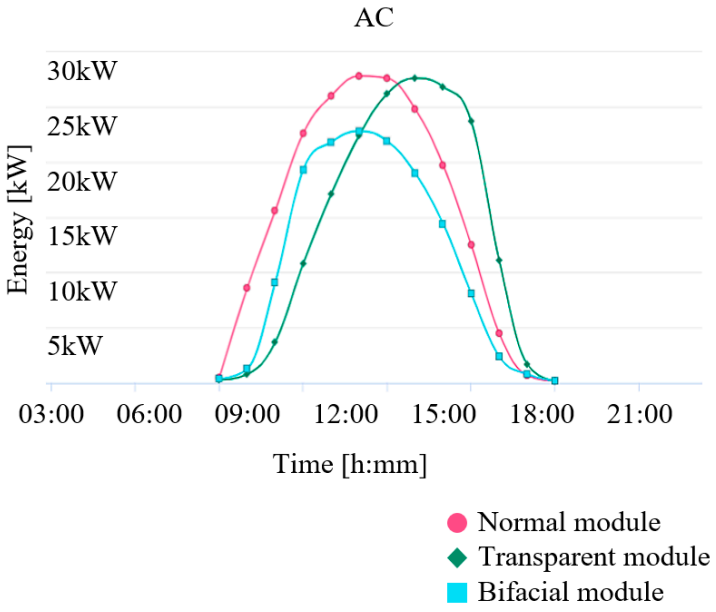

Figure 15. AC power-generation monitoring graph.

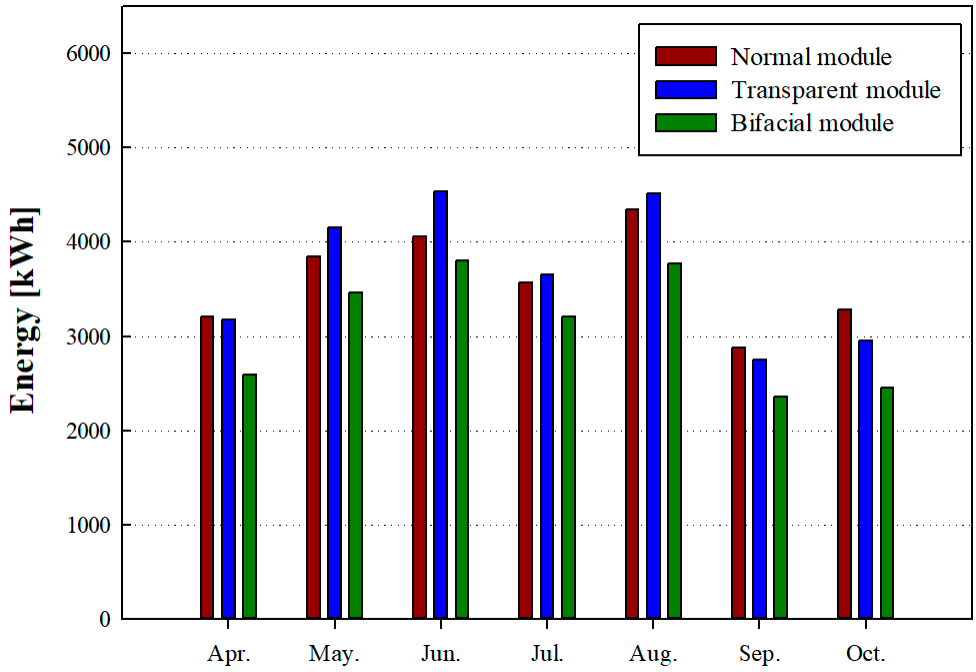

Figure 16. Generated energy of each module per month.

The commercial operation of the agrivoltaic plant started in April 2019. Table 1 shows the daily average and monthly generation amount (KWh) and electricity-price (system marginal price, SMP) income-to-power purchase agreement during the five months. However, this power plant was built for research purposes, so there was no renewable-energy-certificate (REC) profit.

3.2. Growth-Environment Analysis

The data collected from the crop-growth environment sensor included insolation, temperature of the top and bottom layers of the module, soil temperature, and soil-moisture level. We compared the growth environment (carbon dioxide, illuminance, and soil temperature) of the farmland with installed solar panels and without solar panels using the collected data. The growth-environment data of Figures 17–19 were collected from Section D.

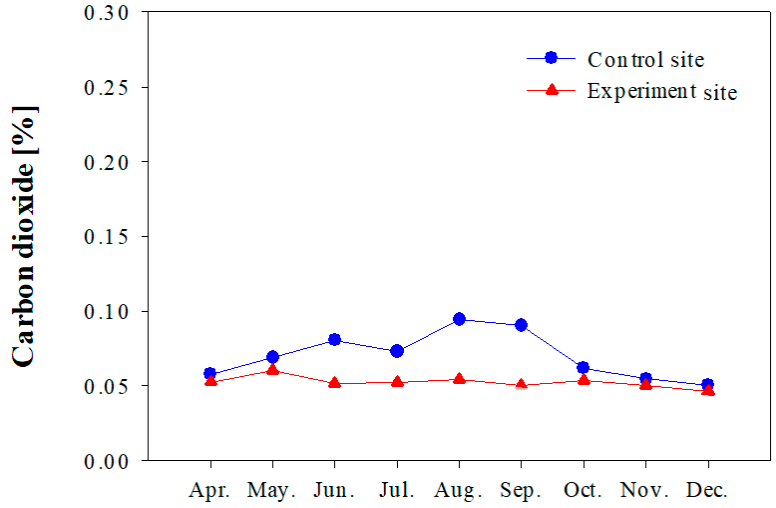

Figure 17. Carbon dioxide level comparison.

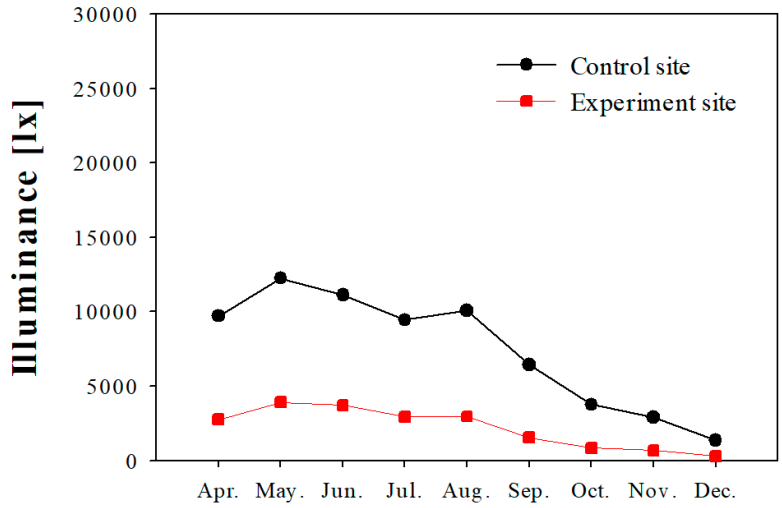

Figure 18. Illuminance comparison.

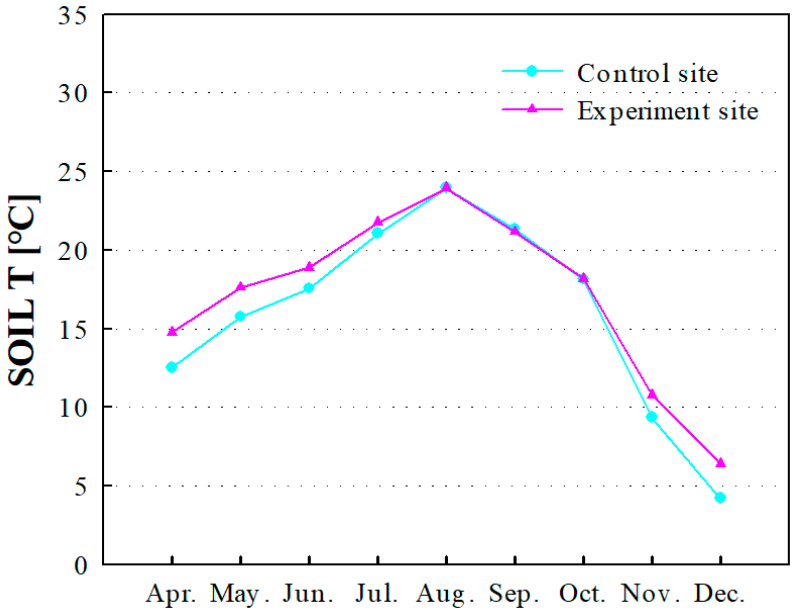

Figure 19. Temperature comparison.

Carbon dioxide (CO_2) level data obtained from the experiment site with the solar panels and the control site without the panels were compared. The average CO_2 level from the control site was 0.09%, and the maximum was 0.17% in July and August. On the other hand, the CO_2 level of the experiment site was 0.05% on average and 0.07% at its peak throughout the year. Moreover, CO_2 is used as fuel for photosynthesis, and plants generally have a 0.003–0.01% CO_2 compensation point and 0.21–0.3% CO_2 saturation point. The minimum CO_2 level is represented by the CO_2 compensation point, where the generation speed of organic matter from photosynthesis matches the consumption speed of organic matter from breathing.

Figure 17 shows the change in monthly CO_2 levels. The difference in CO_2 level between the control and experiment sites was observed, with a minimum CO_2 level of 0.05% detected at the experiment site.

Another environmental factor is the comparison of illuminance between the control and experiment sites. In the control site, the highest illuminance was observed in May at an average of 12,252 lx, with a maximum value of 38,368 lx. The lowest illuminance was in December at an average of 1349 lx, reaching a maximum value of 6203 lx. In the agrivoltaic system, on the other hand, highest illuminance was observed in May at an average of 3905 lx with a maximum value of 19,799 lx. Further, the lowest illuminance was in December at an average of 295 lx with a maximum value of 1946 lx. Lastly, grape luminosity for maximum photosynthesis is 30,000–40,000 lx, meaning that the control site provided enough illuminance for maximum photosynthesis from April to September. However, in the agrivoltaic system, only 50% of maximum photosynthesis occurred from April to September. This lack of photosynthesis slowed grape growth by about 10 days.

Soil temperature is one of the most important factors affecting soil nutrients, and soil-moisture density and viscosity.

As shown in Figure 11, the soil temperature of the control and experiment sites only had minor difference. Figure 19 compares the soil characteristics between the experiment site with solar panels and the control site without panels. On this basis, farmland-soil temperature is an important factor for crop growth, as the dissolution level of land nourishment accordingly changes, directly affecting crop growth. The reason that the temperature was measured as higher in the test site than in the controlled site is due to the temperature rise in the panel during power generation and the fact that it blocks cold air. Despite the shade created by the panel, the temperature did not decrease, but rather rose. The panel is expected to be applied more effectively in cold climates where a temperature increase is required.

The soil temperature of the control site was at its peak in August at an average of 23.94 °C, maximum of 24.87 °C, and minimum of 23.06 °C, and at its lowest in December at an average of 4.16 °C, maximum of 4.75 °C, and minimum of 3.60 °C. In contrast, the soil temperature of the experiment site was at its peak in August, showing an average of 23.94 °C, maximum of 24.48 °C, and minimum of 23.06 °C, and at its lowest in December showing an average of 6.38 °C, maximum of 6.90 °C, and minimum of 5.88 °C. The maximum temperature of the control and experiment sites was similar; however, the minimum temperature of the experiment site was higher than that of the control site by approximately 2 °C. The optimal soil temperature for grape-root generation is in the range of 23–28 °C, indicating that the soil temperature of the control and experiment sites was suitable—no significant difference in grape root generation was observed for temperatures within this range.

However, in April, when germination occurs, the soil temperature of the control site was at an average of 12.52 °C, maximum of 14.70 °C, and minimum of 10.31 °C, and the soil temperature of the experiment site was at an average of 14.78 °C, maximum of 16.52 °C, and minimum of 13.54 °C, meaning that the soil temperature of the experiment site was approximately 2 °C higher than that of the control site. Grape roots become active when the soil temperature reaches 10–14 °C, and start to germinate when the air temperature reaches 10 °C. The experiment site, having a higher soil temperature by 2 °C in April (germination period), could result in faster grape germination compared

to the control site. The actual grape-germination-period data showed a 1–2-day faster germination of grapes at the experiment site.

3.3. Crop-Impact Analysis

Grape germination under the three types of solar modules occurred on approximately 20 April. The difference in the germination period owing to solar-panel implementation was not visually observable, and it occurred during a similar period. The bud-sprouting period differed, between 1 and 2 days, as compared to in the control site, showing almost no difference between the control site (which had no solar panels) and the site with the solar panels.

Figure 20 shows the state of a flower cluster positioned on a branch after 20 days of bud germination. Each branch had 2 to 3 flower clusters, and the nutritional state of the branch caused any difference in the number of flower clusters. The number and growth of flower clusters between the solar-panel-implemented and control sites did not show any difference.

Figure 20. Grape germination (20 April 2019). (**A**) Normal control site, (**B**) normal solar-panel site, (**C**) bifacial control site, (**D**) bifacial solar-panel site, (**E**) transparent control site, and (**F**) transparent solar-panel site.

We researched the impact on the growth and quality of grapes, and the soil-pollution level of the grape farm due to implementing the normal (Type 1), bifacial (Type 2), and transparent (Type 3) solar panels. Figures 21 and 22 compare grape growth in the control and solar-panel-experiment plots. The top-left picture (A) is the Type 1 control plot, and top-right (B) is the Type 1 experiment plot. The middle-left image (C) is the Type 2 control plot, and the middle-right image (D) is the Type 2 experiment plot. The bottom-left image (E) is the Type 3 control plot, and the bottom-right (F) is the Type 3 experiment plot. Grape berries observed 17 days after pollination showed normal growth, and there was no difference in growth between the control and solar-panel-experiment plots.

Figure 23 shows grapes harvested on 28 August to examine pericarp coloration. As compared to the control site, pericarp coloration under the solar-panel module showed a 7–10 days delay in coloration. As the coloration of Campbell Early is related to light, the delay in grape coloration under the experiment site, as compared to the control site, may have occurred because of the difference in luminous intensity.

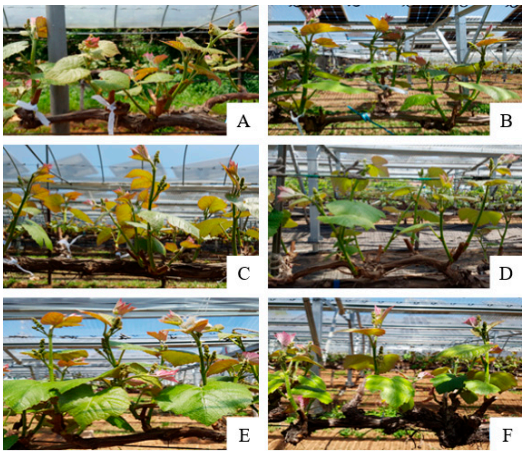

Figure 21. Development changes of grape flower gardens (6 May 2019). (**A**) Normal control site, (**B**) normal solar-panel site, (**C**) bifacial control site, (**D**) bifacial solar-panel site, (**E**) transparent control site, and (**F**) transparent solar-panel site.

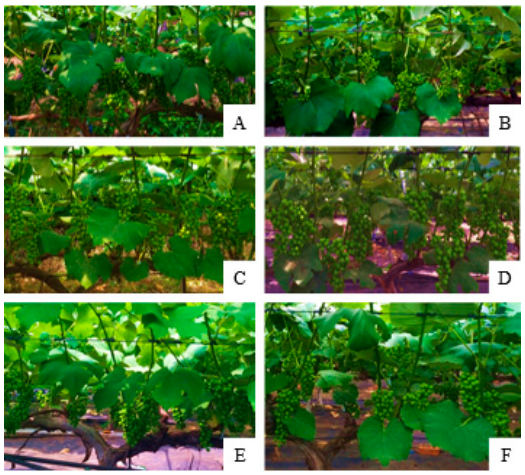

Figure 22. Development status of grape granules according to solar-module installation. (**A**) Normal control site, (**B**) normal solar-panel site, (**C**) bifacial control site, (**D**) bifacial solar-panel site, (**E**) transparent control site, and (**F**) transparent solar-panel site.

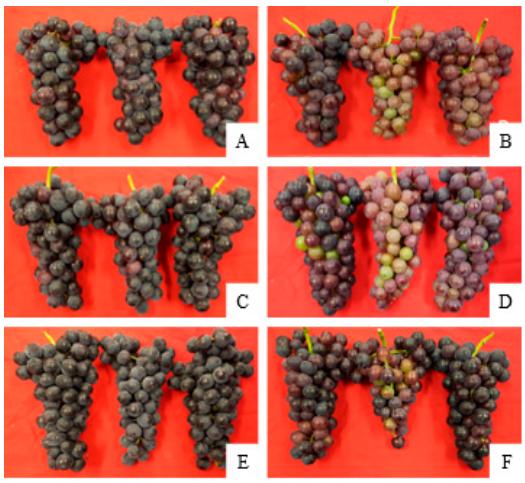

Figure 23. Changes in grape color with PV module sections B/D/F—delay in coloration. (**A**) Normal control site, (**B**) normal solar-panel site, (**C**) bifacial control site, (**D**) bifacial solar-panel site, (**E**) transparent control site, and (**F**) transparent solar-panel site.

Table 2 compares the characteristics of grapes from the control and experiment sites, harvested on 28 August. Grape samples were collected from 1 grape to 10 granules, and from 1 tree to 10 grapes; three trees were targeted in each section. The average sugar content of 300 granules in each section was compared. Letter a~d means in a row by different superscripts are significantly different at 5% significance level by Duncan's multiple range test. Letter a is significant to b, c but "a" and "ab" is not significant.

Table 2. Grape-growth results by photovoltaic (PV) module type.

PV Module Type	Granule Weight	Sugar Content (Brix)	Granule Quantity	Length (mm)	Width (mm)
Without module (Section A)	5.7 ± 0.9 a [1]	13.5 ± 0.8 b	66.4 ± 11.0 bc	21.4 ± 1.3 a	20.2 ± 1.3 a
Normal (Section B)	5.4 ± 0.8 c	12.9 ± 1.8 bc	58 ± 13.1 c	20.9 ± 1.0 ab	19.9 ± 1.2 ab
Without module (Section C)	5.1 ± 0.6 ab	13.4 ± 0.9 bc	68.4 ± 5.2 bc	20.7 ± 0.9 bc	19.6 ± 0.8 abc
Bifacial (Section D)	5.0 ± 0.5 bc	12.7 ± 0.8 c	73 ± 5.4 b	20.7 ± 0.7 bc	19.3 ± 0.7 bc
Without module (Section E)	4.9 ± 0.8 ab	15.4 ± 0.9 a	70.8 ± 12.3 bc	20.0 ± 1.1 ab	19.0 ± 1.2 c
Transparent (Section F)	4.2 ± 0.6 ab	11.3 ± 0.9 d	89.8 ± 6.9 a	19.5 ± 1.1 a	18.1 ± 1.0 d

a [1], mean separation within each column by Duncan's multiple range test, 5% level.

The distinctive factor is that fruits under solar-panel modules showed slower growth than those at the control site. The relevance of sugar-concentration level was observable where fruits in the experiment site had lower sugar concentrations than those at the control site. As shown in Figure 23, this result concurs with the fact that lower sugar concentration was observed in grapes under solar-panel modules, which had a delay in coloration.

Figure 24 shows the results of examining changes in skin coloration according to each solar module by second-harvest grapes, 10 days after the first harvest. The coloration of grape skins grown in each solar module site was not different compared to that in the control site. In the early stages of harvest, bark coloration was less well-formed than that in the control site, but there was no color difference in the maturity period.

Figure 24. Changes in grape color with PV modules—no difference in coloration in all sections. (**A**) Normal control site, (**B**) normal solar-panel site, (**C**) bifacial control site, (**D**) bifacial solar-panel site, (**E**) transparent control site, and (**F**) transparent solar-panel site.

Table 3 shows the sugar-concentration levels of grapes harvested during the full ripe period in the control and experiment groups. Measurement of the Brix degree of late-harvest grapes showed similar values between the control group and those under normal, bifacial, and transparent solar-panel

modules. This implies that the grapes under solar panels had slower growth, but their quality could be maintained by controlling the harvesting period. Further research is planned for cyclical testing in 2020.

Table 3. Changes in sugar content according to PV module in ripe grapes.

PV Module Type	Division	Sugar Content (Brix)
Normal	Without module (A)	17.5
	With module (B)	18.6
Bifacial	Without module (C)	16.7
	With module (D)	17.1
Transparent	Without module (E)	17.3
	With module (F)	17.1

4. Conclusions

This study compared the crop-growth environment in a rain-hit-protection facility with a solar-power system to a facility without solar panels. Then, effects on growth and power-production profit were analyzed.

Soil temperature in the test site was higher in spring and winter compared to in the control site. In particular, the test-site soil temperature in April was 14.78 °C on average, 2.26 °C higher than that in the control site, and the germination of the test-site grapes in April was one to two days faster than that of grapes in the control site. On the other hand, the coloring and growth of the test-site grapes was delayed compared to those of grapes in the control site. This was due to a combination of solar-radiation reduction and temperature changes caused by the installation of solar modules. Grapes of the first harvested test site showed lower quality than those of the control site with regard to weight and sugar content. Considering the delayed growth of the grapes in the test site, the second harvest was performed 10 days after the first harvest. The quality of the second harvested test-site grapes was similar to that of the first harvested control-site grapes. This means that it is possible to cultivate high-quality crops by only changing harvest time at the solar-power facility. Three types of solar panels (normal, bifacial, and transparent panels) were used for the study, but no significant difference was found in their effect on power generation and grape growth. There was a profit of USD 5551 related to the power transaction, and 55 MWh was produced during the five months that grape growth was monitored.

This study confirmed that the mutual coexistence of agriculture and renewable energy is possible by utilizing solar-power systems as a crop-cultivation environment. We will conduct it again for the verification of the relationship between solar power and grape growth in 2020. Other crop studies, such as for cabbages and onions, are also being conducted. This study may serve as a basis for further research on the coexistence of renewable energy and agriculture.

Author Contributions: Conceptualization, J.C. and I.-H.R.; methodology, J.C. and S.M.P.; software, O.C.L.; investigation, A.R.P.; writing—original draft preparation, J.C. and G.N.; writing—review and editing, J.C. and A.R.P.; supervision, I.-H.R. All authors have read and agreed to the published version of the manuscript.

Funding: This research was funded by the Korean government (MOTIE) [20173010013390].

Acknowledgments: This work was supported by the Korea Institute of Energy Technology Evaluation and Planning (KETEP), grant funded by the Korean government (MOTIE) (20173010013390, development and field testing of 100 kW agro-PV systems) and this work was supported by the Institute for Information and Communications Technology Promotion (IITP) grant funded by the Korea government (MSIT) (No. 2018-0-00508) development of blockchain-based embedded devices and platform for MG security and operational efficiency.

Conflicts of Interest: The authors declare no conflict of interest.

References

1. Kadowaki, M.; Yano, A.; Tanaka Ishizu, F.; Tanaka, T.; Noda, S. Effects of greenhouse photovoltaic array shading on welsh onion growth. *Biosyst. Eng.* **2012**, *111*, 290–297. [CrossRef]
2. Cossu, M.; Murgia, L.; Ledda, L.; Deligios, P.A.; Sirigu, A.; Chessa, F.; Pazzona, A. Solar radiation distribution inside a greenhouse with south-oriented photovoltaic roofs and effects on crop productivity. *Appl. Energy* **2014**, *133*, 89–100. [CrossRef]
3. Kuo, Y.-C.; Chiang, C.-M.; Chou, P.-C.; Chen, H.-J.; Lee, C.-Y.; Chan, C.-C. Applications of building integrated photovoltaic modules in a greenhouse of Northern Taiwan. *J. Biobased Mater. Bioenergy* **2012**, *6*, 721–727. [CrossRef]
4. Shamshiri, R.R.; Weltzien, C.; Hameed, I.A.; Yule, I.J.; Grift, T.E.; Balasundram, S.K.; Pitonakova, L.; Ahmad, D.; Chowdhary, G. Research and development in agricultural robotics: A perspective of digital farming. *Int. J. Agric. Biol. Eng.* **2018**, *11*, 1–14. [CrossRef]
5. Shamshiri, R.R.; Bojic, I.; van Henten, E.; Balasundram, S.K.; Dworak, V.; Sultan, M.; Weltzien, C. Model-based evaluation of greenhouse microclimate using IoT-Sensor data fusion for energy efficient crop production. *J. Clean. Prod.* **2020**, 121303. [CrossRef]
6. Ezzaeri, K.; Fatnassi, H.; Bouharroud, R.; Gourdo, L.; Bazgaou, A.; Wifaya, A.; Demrati, H.; Bekkaoui, A.; Aharoune, A.; Poncet, C.; et al. The effect of photovoltaic panels on the microclimate and the tomato production under photovoltaic Canarian greenhouses. *Sol. Energy* **2018**, *173*, 1126–1134. [CrossRef]
7. Kim, D.; Kim, C.; Park, J.; Kim, C.; Nam, J.; Cho, J.; Lim, C. Computer simulation of lower farmland by the composition of an agrophotovoltaic system. *New Renew. Energy* **2020**, *16*, 41–46. [CrossRef]
8. Gray, M.K.; Morsi, W.G. On the role of prosumers owning rooftop solar photovoltaic in reducing the impact on transformer's aging due to plug-in electric vehicles charging. *Electr. Power Energy Syst.* **2017**, *143*, 563–572. [CrossRef]
9. Luz, T.; Moura, P.; Almeida, A. Multi-objective power generation expansion planning with high penetration of renewables, Renew. *Sustain. Energy Rev.* **2018**, *81*, 2637–2643. [CrossRef]
10. Shang, C.; Srinivasan, D.; Reindl, T. An improved particle swarm optimization algorithm applied to battery sizing for stand-alone hybrid power systems. *Int. J. Electr. Power Energy Syst.* **2016**, *74*, 104–117. [CrossRef]
11. Aroca-Delgado, R.; Pérez-Alonso, J.; Callejón-Ferre, Á.-J.; Díaz-Pérez, M. Morphology, yield and quality of greenhouse tomato cultivation with flexible photovoltaic rooftop panels. *Sci. Hortic.* **2019**, *257*, 108768. [CrossRef]
12. Tsao, T.-F.; Chang, H.-C. Comparative case studies for value-based distribution system reliability planning. *Electric Power Syst. Res.* **2004**, *68*, 229–237. [CrossRef]
13. Dalei, J.; Mohanty, K.B. Fault classification in SEIG system using Hilbert-Huang transform and least square support vector machine. *Int. J. Electr. Power Energy Syst.* **2016**, *76*, 11–22. [CrossRef]
14. Erişti, H.; Yıldırım, Ö.; Erişti, B.; Demir, Y. Optimal feature selection for classification of the power quality events using wavelet transform and least squares support vector machines. *Int. J. Electr. Power Energy Syst.* **2013**, *49*, 95–103. [CrossRef]
15. ElNozahy, M.S.; Salama, M.M.A. Studying the feasibility of charging plug-in hybrid electric vehicles using photovoltaic electricity in residential distribution systems. *Electr. Power Syst. Res.* **2014**, *110*, 133–143. [CrossRef]
16. Kim, K.; Yoon, J.-Y.; Kwon, H.-J.; Han, J.-H.; Son, J.E.; Nam, S.-W.; Giacomelli, G.A.; Lee, I.-B. 3-D CFD analysis of relative humidity distribution in greenhouse with a fog cooling system and refrigerative dehumidifiers. *Biosyst. Eng.* **2008**, *100*, 245–255. [CrossRef]
17. Klaring, H.-P.; Klopotek, Y.; Schmidt, U.; Tantau, H.-J. Screening a cucumber crop during leaf area development reduces yields. *Ann. Appl. Biol.* **2012**, *161*, 161–168. [CrossRef]
18. Park, D.; Kim, M.; So, W.; Oh, S.-Y.; Park, H.; Jang, S.; Park, S.-H.; Kim, W.K. Evaluation of bifacial si solar module with different albedo conditions. *Curr. Photovolt. Res.* **2018**, *6*, 62–67. [CrossRef]
19. Kim, M.; Ji, S.; Oh, S.-Y.; Jung, J.H. Prediction study of solar modules considering the shadow effect. *Curr. Photovolt. Res.* **2016**, *4*, 80–86. [CrossRef]
20. Lee, S.-H.; Oh, H.K.; Lee, K.S. PV System Output Analysis Based on Weather Conditions, Azimuth, and Tilt Angl. *Curr. Photovolt. Res.* **2017**, *5*, 38–42. [CrossRef]

21. Jeong, J.-H.; Lim, C.-M.; Jo, J.-H.; Kim, J.-H.; Kim, S.-H.; Lee, K.-Y.; Lee, S.-S. A study on the monitoring system of growing environment department for smart farm. *J. Korea Inst. Inform. Electron. Commun. Technol.* **2019**, *12*, 290–298. [CrossRef]
22. Yang, Q. Development Strategy of Plant Factory. *Sci. Technol. Rev.* **2014**, *32*, 20–24. [CrossRef]
23. Ureña-Sánchez, R.; Callejón-Ferre, Á.J.; Pérez-Alonso, J.; Carreño-Ortega, Á. Greenhouse tomato production with electricity generation by roof-mounted flexible solar panels. *Sci. Agric.* **2012**, *69*, 233–239. [CrossRef]
24. Nugraha, G.D.; Musa, A.; Cho, J.; Park, K.; Choi, D. Lambda-based data processing architecture for Two-Level load forecasting in residential buildings. *Energies* **2018**, *11*, 772. [CrossRef]
25. Sacchelli, S.; Garegnani, G.; Geri, F.; Grilli, G.; Paletto, A.; Zambelli, P.; Ciolli, M.; Vettorato, D. Trade-off between photovoltaic systems installation and agricultural practices on arable lands: An environmental and socio-economic impact analysis for Italy. *Land Use Policy* **2016**, *56*, 90–99. [CrossRef]
26. Dinesh, H.; Pearce, J.M. The potential of agrivoltaic systems. *Renew. Sustain. Energy Rev.* **2016**, *54*, 299–308. [CrossRef]
27. Cossu, M.; Cossu, A.; Deligios, P. Assessment and comparison of the solar radiation distribution inside the main commercial photovoltaic greenhouse types in Europe. *Renew. Sustain. Energy Rev.* **2018**, *94*, 822–834. [CrossRef]
28. Fukatsu, T.; Kiura, T.; Hirafuji, M. A web-based sensor network system with distributed data processing approach via web application. *Comput. Stand. Interfaces* **2011**, *33*, 565–573. [CrossRef]
29. Ge, J.; Cai, C.; Liu, Y.; Gong, X. Effect of Irrigation Time on the growth rate and indoor environment of greenhouse eggplant. *J. Inst. Eng. (India) Ser. A* **2018**, *99*, 647–651. [CrossRef]
30. Ganguly, A.; Ghosh, S. Model development and experimental validation of a floriculture greenhouse under natural ventilation. *Energy Build.* **2009**, *41*, 521–527. [CrossRef]
31. Yano, A.; Kadowaki, M.; Furue, A.; Tamaki, N.; Tanaka, T.; Hiraki, E.; Kato, Y.; Ishizu, F.; Nodad, S. Shading and electrical features of a photovoltaic array mounted inside the roof of an east-west oriented greenhouse. *Biosyst. Eng.* **2010**, *106*, 367–377. [CrossRef]
32. Gaddam, A. Designing a wireless sensors network for monitoring and predicting droughts. In Proceedings of the 8th International Conference on Sensing Technology, Liverpool, UK, 2–4 September 2014.